CORROSION SCIENCE AND TECHNOLOGY, Vol.9, No.6(2010), pp.247~253

Characterization of the Galvanizing Behavior Depending on Annealing Dew Point and Chemical Composition in Dual-Phase Steels

K.S. Shin†, S.H. Park, S.H. Jeon[1], D.C. Bae[1], and Y.M. Choi[1]

Research Institute of Industrial Science and Technology (RIST), Pohang 790-330, Korea
[1]POSCO Technical Research Laboratories, Gwangyang, 545-090, Korea
(Received August 3, 2009; Revised December 10, 2010; Accepted December 13, 2010)

The characteristics of selective oxidation prior to hot-dip galvanizing with the annealing atmosphere dew point and chemical composition in dual-phase steels and their effect on the inhibition layer formation relevant to coating adhesion have been studied using a combination of electron microscopic and surface analytical techniques. The annealed and also galvanized samples of 3 kinds of Si/Mn ratios with varied amounts of Si addition were prepared by galvanizing simulator. The dew point was controlled at soaking temperature 800 ℃ in 15%H_2-85%N_2 atmosphere. It was shown that good adhesion factors were mainly uniformity of oxide particle distribution of low number density and low Si/Mn ratio prior to hot-dip galvanizing. Their effect was the greatly reduced coating bare spots and the formation of uniform inhibition layer leading to good adhesion of Zn overlay. The mechanism of good adhesion is suggested by two processes: the formation of inhibition layer on the oxide free surface uncovered with no SiO_2-containing particles in particular, and the inhibition layer bridging of oxide particles. The growth of inhibition layer was enhanced markedly by the delayed reaction of Fe and Al with the increase of Si/Mn ratio.

Keywords *: hot-dip galvanizing, coating adhesion, dual-phase steel*

1. Introduction

High strength dual-phase steel(HS-DP) is one of the attractive candidates for lightweight automotive applications due to its high strength and good formability brought about by a complex ferrite-martensite microstructure.[1),2)] For automobile durability by means of corrosion protection, good galvanizability is essentially required. The dual-phase ferrite-martensite microstructure is conventionally obtained by adding the following alloying elements: Mn with Si, Cr, or Al, and an appropriate annealing heat cycle consisting of an intercritical annealing and then rapid cooling in order to transform the intercritical austenite to martensite.[3)-5)] Mn or Cr plays an important role of increasing the strengthening and hardenability as well, and Si or Al is used for solid solution strengthening and suppressing the carbide formation.

However, these alloying elements are known to form selective oxides in surface region in conventional continuous galvanizing line atmosphere, possibly leading to the poor Zn wettability.[6),7)] The reactive wetting of the steel surface by molten Zn is of primary importance for the formation of well-developed inhibition layer and corresponding coating adhesion. In this work, the influence of the annealing atmosphere dew point and chemical composition in dual phase steels on the surface selective oxidations and their effect on the formation of inhibition layer in association with coating adhesion have been studied using electron microscopic and surface analytical techniques. The results of surface chemistry by selective oxidation were interpreted in comparison with those of SiO_2-MnO binary phase diagram.

2. Experiment

Chemical compositions of the 3 steels of Si/Mn mass ratios by a 1.9 wt% Mn-added steel base and varied amounts of Si addition are listed in Table 1. The volume fraction was predicted using database TCFE5 of Thermo-Calc version R. Samples of size 200 mm x 120 mm x 0.8 mm cut from the cold-rolled sheets were annealed in the protective atmosphere of 15 vol% H_2-85 vol% N_2 and galvanized by dipping them into molten Zn containing 0.23 wt% Al using Rhescar hot-dip Simulator. The sam-

† Corresponding author: ksshin@rist.re.kr

Table 1. Chemical compositions of substrate steel used in the present study (in mass %)

steel	C	Mn	Si	P	S-Al	Si/Mn ratio	volume fraction at soaking temperature 800 ℃
No 3	0.08	1.91	0.12	0.018	0.04	0.063	BCC: 0.32; FCC:0.68
No 6	〃	1.91	0.50	〃	〃	0.26	BCC: 0.41; FCC:0.59
No 7	〃	1.88	0.97	〃	〃	0.52	BCC: 0.54; FCC:0.46
pH_2O/pH_2 on dew points -60 ℃, -40 ℃, -20 ℃, and 0 ℃ : 0.0000107, 0.000126, 0.00102, and 0.00603							

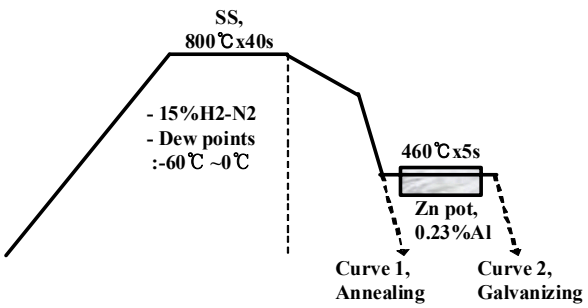

Fig. 1. Schematic illustration of heat treatment cycle for annealing and galvanizing process for HS-DP steels.

ples were heated to 800 ℃ at soaking section(SS) and maintained for 40s following rapid cooling to room temperature(curve1 in Fig. 1) or continued to dipping in Zn bath(curve 2 in Fig. 1). The application of 4 kinds of dew points (DPs: -60 ℃, -40 ℃, -20 ℃, 0 ℃) were performed during annealing cycle.

Surface chemistry of alloying elements was characterized by a combination of glow discharge spectrometer (LECO 850A, GDS) and Fourier transform infrared spectrometer (Shimadzu IRPrestige-21, FT-IR). Surface morphologies of external oxidation were also analyzed by FE SEM (JEOL JSM-6700F, cold FEG gun). GDS and FE- TEM (JEM 2100F FE TEM, JEOL) were employed to provide the information on the characters of inhibition layer structure. In the GDS analyses of inhibition layer, Zn-Fe intermetallics as well as pure Zn coating was removed by chemical dissolution procedure in a solution of distilled water 95 ml, HNO_3 5 ml, CrO_3 20 g, and $ZnSO_4$ 4 g. The specimen for FE TEM was prepared in thin foil by the application of focused ion beam (SMI3050SE FIB/SEM, Seiko). The adhesion quality of Zn coating was further confirmed by 0t-bending test and macro-photograph of outer bended surface.

3. Results and discussion

3.1 Surface morphologies and chemistry after annealing cycle

The dependence of surface morphologies on Si/Mn ratios and annealing dew points was first investigated. Fig. 2 shows representative observations with the change of chemical compositions at -60 ℃ dew point by FE SEM. The surface of steel No 3 shows the fairly uniform distribution of nodular particles of ~100 nm size by selective external oxidation. No continuous oxides exist along grain boundary. In contrast in the case of steel No 6, the size distribution of oxide particles was non-uniform, grain boundary oxidation developed in occasional continuity of line-type and nodular oxides, and oxides of net type sporadically formed at the free surface, inside the grains. The surface morphology of steel No 7 is analogous to that of steel No 6 except for the absence of oxides of net type

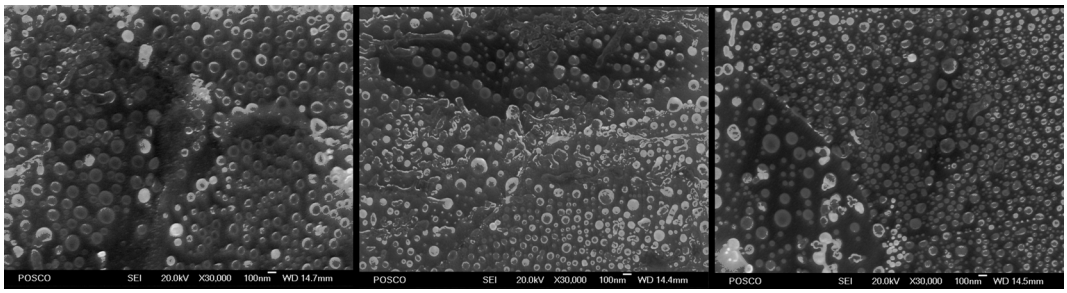

(a) Si/Mn = 0.063 (b) Si/Mn = 0.26 (c) Si/Mn = 0.52

Fig. 2. Effect of Si content on the surface morphology by selective oxidation of HS-DP steels after annealing in the -60 ℃ dew point atmosphere under 15%H_2-N_2 at 800 ℃ for 40s: (a) steel No 3, Si/Mn=0.063; (b) steel No 6, Si/Mn=0.26; (c) steel No 7, Si/Mn=0.52.

and the high-density distribution of surface oxides with a wide range of particle size. The notable difference in particle density between grains is presumably related to crystallographic anisotropy. The common aspect of surface oxidation of 3 steels is that there is free surface uncovered by selective oxides, which can give rise to the good wettability of molten Zn.

The continuous oxidation along grain boundary can be accounted for by the increased Si in steel No 6 and 7. This is because Si-related oxides, SiO_2 or Mn-Si complex oxides, are apt to form by compact film type rather than by particle-like shape due to their role of diffusion barrier to oxygen and metal ions during annealing cycle.[8] During intercritical annealing, diffusion coefficient of Si is much higher in g-phase than that of Mn,[9] so that its segregation through easy diffusion path via grain boundary will become accelerated, leading to the formation of continuous oxide. On the other hand, Mn-rich oxide is known to grow in particle-like form with its less compactness[8] and this feature is evidenced in Fig. 2(a) showing the uniform distribution of surface oxides. Additionally, a mixture of various Si and Mn-Si oxides is probably in association with the non-unifomity of surface oxide distribution as shown in Fig. 2(b) and (c). The density of particle distribution with the increase of dew point becomes low because of the internal oxidation.

Fig. 3 shows the typical GDS in-depth profile of annealed steel No 6 demonstrating the obvious difference in surface selective oxidation with the change of dew point. The -20 DP annealed sample had much less amounts of Mn and Si surface segregation as well as much thinner oxidation than the -60 DP sample. The result was attributed to the internal oxidation in the form of Mn-Si-Al-O compounds at high dew point of annealing atmosphere.

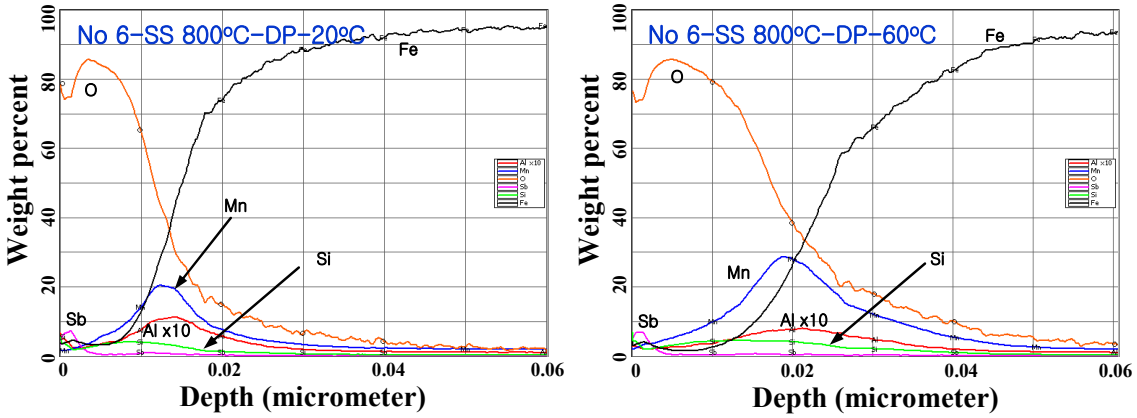

Fig. 3. GDS in-depth composition profile of steel No 6 in the -20 ℃ and -60 ℃ dew point atmospheres at 800 ℃ soaking temperature.

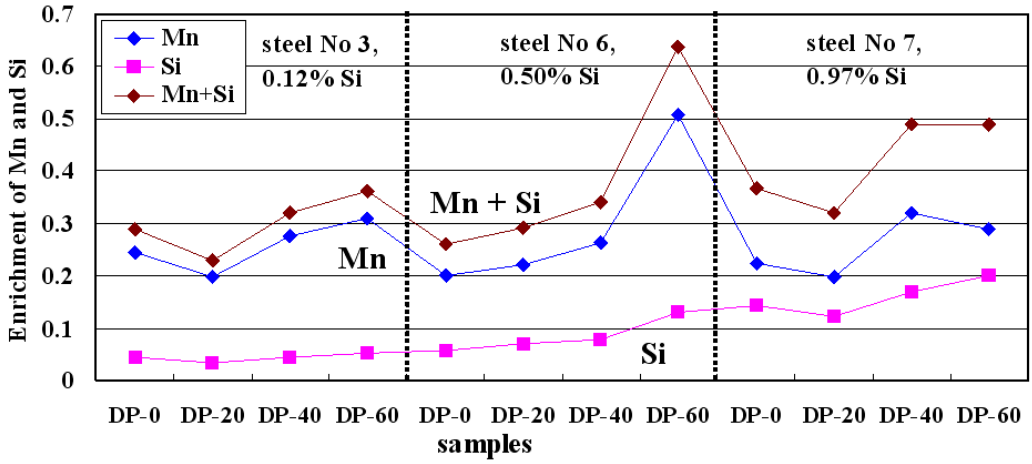

Fig. 4. The behavior of Mn and Si surface enrichment of 3 HS-DP steels according to dew points 0 ℃, -20 ℃, -40 ℃, and -60 ℃. The elemental enrichment is refered to as the integral (μm*wt%) from the surface up to the depth of 80 wt% Fe in GDS depth compositional profile.

This situation generally applied to the other samples. Based on the GDS in-depth compositional profile, the enrichment behavior of Mn and Si was further studied in order to obtain better insight of the dependence of surface enrichment on the Si/Mn ratios and annealing dew points as shown in Fig. 4.

Fig. 4 depicts the tendency toward the amounts of surface enrichment. It can be seen with some exceptions that Si segregation monotonously increases with the decrease of dew points and the increase of Si addition, whereas the behavior of Mn segregation resembles each other for separate steels, not accompanying the overall increasing character of Si enrichment. The simply increasing enrichment of Si is due to the fact that the low dew point makes internal oxidation less considerable and in addition Si and Mn can produce stable oxides together. The standard free energies (kJ/mol, 800 ℃) of formation of the oxides per mole oxygen as the parameter of oxide stability are 614, 719, 889, 662, 641 for MnO, SiO_2, Al_2O3, $MnSiO_3$ (2Mn + $2SiO_2$ + O_2), and Mn_2SiO_4 (2Mn + SiO_2 + O_2), respectively.[10] In consequence, Si can form a simple oxide of SiO_2 or Mn-Si complex compounds. The formation of Mn-Si compounds via attractive interaction is more favorable energetically, providing that there are sufficient outward flux of Mn and Si, and dissolved oxygen available on the surface during annealing atmosphere. As for the Mn enrichment, steel No 3 shows moderate increase with the lowering of dew points and steel No 6 slightly suppressed increase at high dew points but steep rise at -60 DP primarily by the enhancement of outward Mn and Si diffusions. Steel No 7 demonstrates similar behavior to steel No 3 implying that the increased Si enrichment would probably lead to the formation of simple oxides of SiO_2. The rising of concurrent enrichment of Si and Mn at 0 ℃ DP of steel No 3 and 7 may be related to inter-alloy element interactions, difference in surface defects such as dislocation, subboundary etc. during heat treatment, or decarburization enhancing the surface segregation by the reduction of inward oxygen diffusion, and remains to be investigated further.

Chemical species of the surface oxides were identified using FT-IR measurements, and their results were compared with those predicted in the SiO_2-MnO binary phase diagram by the surface enrichment of Si and Mn of GDS in-depth profile. The Fig. 5(a) presents the dependence of variation of infrared absorbance of SiO_2, $MnSiO_3$, and Mn_2SiO_4 on dew points and Si/Mn ratios. In the case of low Si/Mn ratio 0.06, the peaks of Mn-Si compounds exhibit somewhat insensitive behavior to the change of dew point. The intensity of Mn_2SiO_4 at -60 ℃ DP and Si/Mn ratio 0.26, however, is clearly enhanced due to the suppression of internal oxidation leading to the notable elevation of Mn and Si enrichment as can be seen in Fig. 4. When the Si/Mn ratio approaches to 0.56, new chemical state of SiO_2 develops by the increased Si addition, and the strong intensity of Mn_2SiO_4 at 0 DP becomes weak with the lowering of dew point because of the corresponding increase of the intensity of $MnSiO_3$ peak.

The possible chemical states of selective oxides are predicted in the SiO_2-MnO phase diagram of Fig. 5(b) using the mole fraction, $SiO_2/(SiO_2+MnO)$, obtained from the results in Fig. 4. When the Si/Mn ratio is low at 0.06,

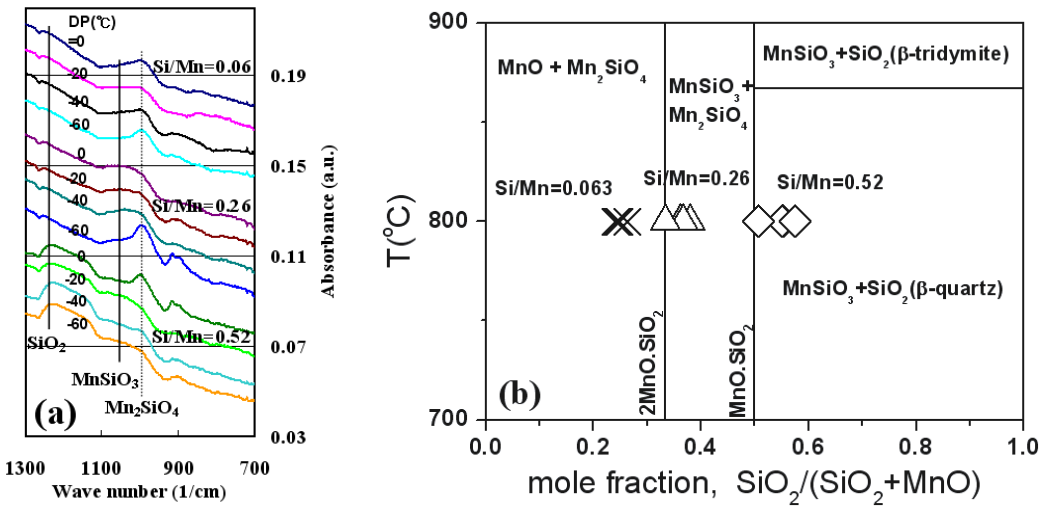

Fig. 5. (a) FT IR measurements and (b) binary phase diagram for SiO_2-MnO obtained by FactSage with the data points from the surface enrichments of Si and Mn of GDS depth profile indicated as crosses, triangles, and diamonds for 3 steels with the variation of dew point and Si/Mn ratio at 800 ℃ soaking temperature.

MnO and Mn_2SiO_4 can coexist, which does not coincide with the FT-IR measurements. The disagreement indicates that the data from phase diagram is lacking in support as a guideline for the experimental results. This is very likely due to the fact that thermodynamic equilibrium phases can not generally be consistent with the surface selective oxides produced kinetically as a function of elemental diffusivities, oxide stability, and oxide solubility especially during intercritical annealing. But, the MnO predicted in phase diagram may form actually in contradiction to FT-IR measurements, because FT-IR is not sensitive to the detection of surface selective oxidation in comparison with surface sensitive X-ray photoelectron spectroscopy (not applied in this work). Recently, the elaborate calculations taking account of the the above parameters are reported, and their predictions are expected to bring the suitable information in assistance to the experiment.[11),12)] In the case of Si/Mn ratio 0.26, the mixture of $MnSiO_3$ and Mn_2SiO_4 in the phase diagram is in good agreement with the FT-IR results. When the Si/Mn ratio is high at 0.52, the phase diagram predicts the observed oxides from FT-IR qualitatively well except for Mn_2SiO_4 oxide.

3.2 Formation of inhibition layer and its effect on coating adhesion for galvanized steels

The galvanizability is determined by the visual appearance of galvanized or galvannealed sheets, by observing the reaction products in Fe-Zn interface, and by the improvement of galvannealing rate.[13)-15)] The good reactive wetting in Zn bath gives rise to the reduced bare spots and well-developed interfacial inhibition layer relevant to good adhesion quality. It is well known that the wettabilty of molten Zn is more greatly deteriorated by selective oxide SiO_2 than Mn-Si-O complex compounds.[12)] The coating quality is assessed by measuring the coating bare spots and also the coating adhesion in high strength steels.

Regarding the visual inspection of galvanized steel(not shown here), the No 3 and 6 steels demonstrated good wettability with rare bare spots being detected, whereas steel No 7 of high Si addition resulted in the frequent development of local bare spots of ~200 μm size. In order to reveal the dependence of the average enrichment of Fe, Al, and Zn on the dew points and Si/Mn ratios in inhibition layer, the integral compositions in GDS measurements are presented in Fig. 6. In the case of steel No 3, the enrichment comprising Fe and Al with small amount of Zn is nearly independent of the dew points. Interestingly, there exists generally monotonous increase of the enrichment with the lowering of dew point and the increase of Si/Mn ratio in the range of 0.26~0.52. The involvement of element Zn implies that the composition cab be $Fe2Al_{5-x}Zn_x$

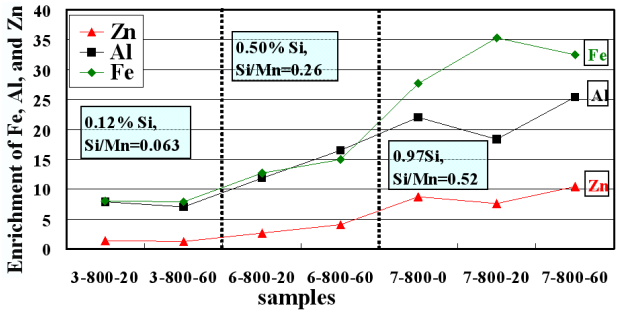

Fig. 6. The behavior of Fe, Al, and Zn enrichment in the interfacial reaction product of Fe-Zn interface for 3 HS-DP galvanized steels with the variation of annealing dew points after stripping the Zn overlay. The elemental enrichment is referred to as the integral (μm*wt%) from the surface up to the depth of 84 wt% Fe in GDS depth compositional profile. The exemplary note of sample, 3-800-20, refers to steel No3, SS 800 ℃, and -20 ℃ DP.

typical of the structure of inhibition layer.[14)] It is important to note that this tendency toward the compositional segregation in inhibition layer does not have analogy to Mn segregation by surface oxidation during annealing, but corresponds well to the tendency toward Si surface segregation, as can be seen in Fig. 4.

In order to obtain the better understanding of the microstructure of interfacial inhibition layer, FE-TEM analysis was performed for the FIB cross-sections of galvanized sheet of no bare spot including the Zn-Fe interface. The Fig. 7 depicts the structural characteristics of the inhibition layer Fe-Al-Zn, Zn-Fe intermetallics, selective surface oxides remaining after galvanizing, and internal oxides for galvanized steel No 3 and 7 annealed at -60 ℃ dew point. In the case of steel No 3, the inhibition layers by the reactive wetting of oxide free surface and on the nodular oxide particles were coupled to form the well-developed 2-dimensional film of thickness ~100 nm. As for the steel No 7, however, there were reaction products composed of inhibition layer Fe-Al-Zn and Zn-Fe-(Al) intermetallics as well in the Zn-Fe interface. The inhibition layer was non-uniform in thickness of several hundreds nm and also somewhat discontinuous, resulting in no good inhibition formation.

The standard free energies (kJ/mol, 460 ℃) of formation of the oxides per mole of oxygen are 666, 779, 964, 759, 740 for MnO, SiO_2, Al_2O_3, $MnSiO_3$, and Mn_2SiO_4, respectively.[10)] Consequently Al in the Zn bath can possess the thermodynamic driving force to reduce the above surface selective oxides except Al_2O_3. The tendency toward the reducing reaction by Al is expected to be in the order of MnO, Mn_2SiO_4, $MnSiO_3$, and SiO_2, when taking into account the free energies. It has been reported recently that MnO oxide of high Mn dual phase steel is reduced

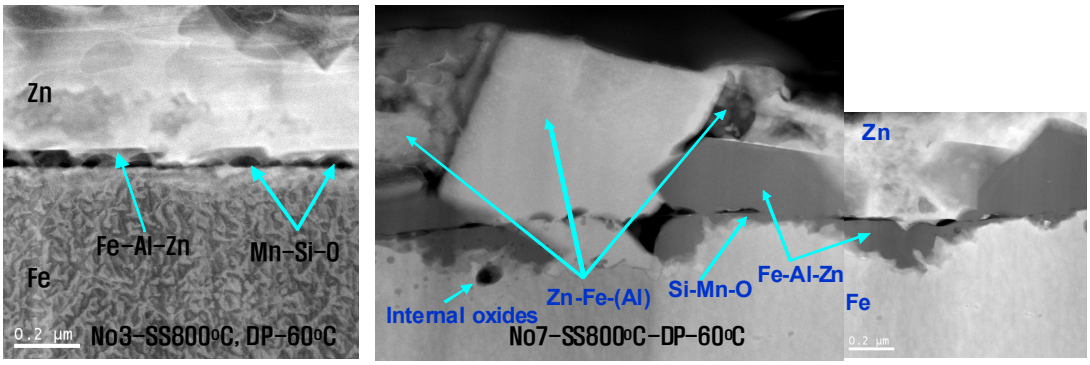

Fig. 7. The microstructure of the interfacial inhibition layer of Fe-Zn interface for No 3 and 7 samples annealed at -60 ℃ DP and galvanized using FE TEM with FIB cross-sections sample preparation.

by the aluminothermic reduction by Al during galvanizing, leading to good reactive wettability.[13] Based on the assumption that surface oxides prior to hot-dip galvanizing can be reduced to some extent in Al-containing Zn bath, Al will be consumed in the reduction reaction of the oxides, which can create a local region in lack of Al in the stagnant Zn bath. The Al depletion in the region very close to steel surface can bring about the formation of incomplete inhibition layer, i.e. inhibition breakdown.[14]

When the Si/Mn ratio is high at 0.52 like steel No 7, however, the resultant surface oxides mainly consist of SiO_2 and Mn-Si-O compounds with high density of oxide distribution, as shown in FE SEM and FT- IR analyses. They will be more difficult to be reduced compared to those of steel No 3 and 6. It is likely then that this situation will leave a local region of Al accumulation adjacent to the steel surface enriched especially with SiO_2. The oxides are generally observed in 2 types of nodule and ultra-thin film on the surface annealed at reducing atmosphere. The distribution of nodular oxide particles can be seen in Fig. 2, and the oxides of inhomogeneous ultra-thin film exist on the free surface uncovered by oxide particles. The Al accumulation will delay the reaction between the steel substrate and the Al resident in the Zn bath, and eventually it is possible that more amounts of the enrichment of Fe, Al, and Zn or thicker inhibition layer will take place in agreement with the observations as shown in Fig. 6. In the meantime, feasible reduction of surface oxides by Al will give rise to the creation of Al depletion zone, where inhibition breakdown can be generated with the formation of Zn-Fe intermetallics instead as shown in Fig. 7. The bare spots observed for steel No 7 are very likely due to the bad reactive wettability by the selective surface oxides. The external oxides will exist in a mixture of SiO_2 and Mn-Si-O compounds of very high-density distribution of inhomogeneous particles locally segregated and also enriched with SiO_2.

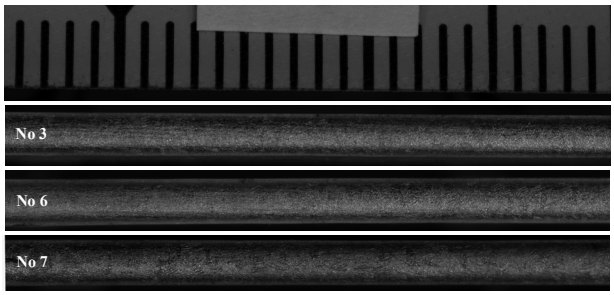

Fig. 8. Macrophotographs of the outer surface after 0t-bending testing of the No 3, 6, and 7 samples annealed at -60 ℃ DP and galvanized.

The adhesion quality was examined by 0t-bending test, and the typical macrophotographs of the outer surfaces are shown in Fig. 8. It can be seen that indeed, the Zn overlay did not exhibit any cracking or splitting for steel No 3 and 6, but revealed the fine surface cracking frequently observable for steel No 7. In addition, it was confirmed that this tendency to adhesion quality was generally independent of the dew points. The quality of no good adhesion of steel No 7 can be explained in a viewpoint of the fact that the fine cracking would be initiated at the Zn-Fe intermetallics, interface between thick inhibition layer and nodular oxide or discontinuity of inhibition layer in the Zn-Fe interface. The inhibition layer bridging of the oxide particles could sustain the adhesion force between oxides and inhibition layer.

4. Summary

In summary, selective oxidation prior to galvanizing with the annealing atmosphere dew point and Si/Mn ratio for dual-phase steels and its effect on the inhibition layer formation and coating adhesion have been studied. It was

confirmed that good adhesion factors in hot dip galvanizing were physical uniformity of oxide particle distribution of low number density and chemically low Si segregation or low Si/Mn ratio prior to hot-dip galvanizing. The influence of dew point on adhesion was very likely insensitive in comparison with the chemical compositions of steels. The good attributes of the selective surface oxidation gave rise to greatly reduced coating bare spots, uniform inhibition layer leading to good adhesion quality by good reactive wetting.

The mechanism of good adhesion is suggested by two processes: the formation of inhibition layer on oxide free surface uncovered with no SiO_2-containing particles in particular, and inhibition layer bridging of oxide particles. The growth of inhibition layer was enhanced markedly by the delayed reaction of Fe and Al with the increase of Si/Mn ratio. It is possibly due to the high density of selective oxidation and weak driving force of Al in molten Zn to reduce surface oxides. In addition, it is surmised that the inhibition layer bridging of oxide particles is deteriorated by the weakened adhesion force between inhibition layer and oxides in high Si/Mn ratio steel.

References

1. B. Mintz, *Int. Mater. Rev.*, **46**, 169 (2001).
2. R. Bode, M. Meurer, T.W.Schaumann, and W.Warnecke, Galvatech'04 Conf. Proc., p. 107 (2004).
3. K. Yosie, JSAE '04 conf. Proc., Society of Automotive Engineers of Japan, Tokyo, 81-4, 29 (2004).
4. Y. Omiya and M. Kamura, *Kobe Steel Engineering Report Tech. Rep*., **52**, 10 (2002).
5. Y. Tobiyama, I. Ozawa, and K. Hirata, *Kawasaki Steel Tech. Rep*., **31**, 181 (1999).
6. R. Khondker, A. Mertens, and J. R. McDermid, *Mater. Sci. Eng. A*, **463**, 157 (2007).
7. E. M. Bellhouse, A.I.M. Mertens, and J.R. McDermid, *Mater. Sci. & Engineering A*, **463**, 147 (2007).
8. Y. Suzuki, Y. Sugimoto, and S. Fugita, Tetsu-to-hagane, **93**, 489 (2007).
9. Ramadeva Shastry, John A. Rotole, and Thomas W. Kaiser, Galvatech'07 Conf. Proc., p. 403 (2004).
10. E. T. Turkdogan, "Physical chemistry of high temperature technology", Academic press, 1980.
11. D. Huin, P. Flauder, and J.-B. Leblond, *Oxidation of Metals*, **64**, 131 (2005).
12. Y. Susuki, *ISIJ Int.*, **49**, 564 (2009).
13. E. M. Bellhouse, A. I. M. Mertens, and J. R. McDermid, *Mater. Sci. Eng. A*, **463**, 147 (2007), R. Khondker, A. Mertens, and J.R. McDermid, *ibid*, 157.
14. E. M. Bellhouse and J. R. MvDermid, *Mater. Sci. Eng. A*, **491**, 39 (2008).